Synthesis, Characterisation, and in vitro Cytotoxic Activity of Dithiocarbamato Glycoconjugate Half-Sandwich Ruthenium and Osmium Complexes

Joan Soldevila-Barreda, Andrea Pettenuzzo, Maria Azmanova, Laia Rafols, Amr Attia, Alexandru Lupan, Luca Ronconi, Nicolas Barry, Anaïs Pitto-Barry

doi.org/10.1002/hlca.202300064

RESEARCH ARTICLE

HELVETICA chimica acta

Synthesis, Characterisation, and *in vitro* Cytotoxic Activity of Dithiocarbamato Glycoconjugate Half-Sandwich Ruthenium and Osmium Complexes

Joan J. Soldevila-Barreda[+],[a] Andrea Pettenuzzo[+],[b] Maria Azmanova,[a] Laia Rafols,[a] Amr A. A. Attia,[c] Alexandru Lupan,[c] Luca Ronconi,*[b] Nicolas P. E. Barry[#],*[a] and Anaïs Pitto-Barry*[a, d]

[a] School of Chemistry and Biosciences, University of Bradford, UK-BD7 1DP Bradford, United Kingdom
[b] School of Biological and Chemical Sciences, University of Galway, IE-H91 TK33 Galway, Ireland, e-mail: luca.ronconi@universityofgalway.ie
[c] Facultatea de Chimie şi Inginerie Chimică, Universitatea Babeş-Bolyai, RO-400028 Cluj-Napoca, Romania
[d] Université Paris-Saclay, CNRS, Institut Galien Paris-Saclay, FR-91400 Orsay, France, e-mail: anais.pitto-barry@universite-paris-saclay.fr

Dedicated to Prof. *Robert Deschenaux* on the occasion of his 65th birthday

The synthesis by transmetallation and in-depth characterisation by IR spectroscopy of five half-sandwich ruthenium and osmium dithiocarbamato isonipecotamide glycoconjugate complexes are presented herein. The evaluation of their *in vitro* cytotoxicity and of the zinc precursors' *in vitro* cytotoxicity towards ovarian cancer (A2780 and A2780cisR) and normal prostate (PNT2) cells is reported. While the cytotoxicity of the compounds is rather limited, some selectivity is observed.

Keywords: cytotoxicity, glycoconjugates, half-sandwich metal complexes, sandwich complexes.

Introduction

Half-sandwich 'piano stool' metal complexes are a particular class of organometallics which has attracted an enormous attention for the design of anticancer drug candidates.[1–4] The synthetic versatility of half-sandwich metal complexes allows modulation of their biological and pharmacological properties by the appropriate choice of the ligands.[2,5–23] Particularly, the choice of the bidentate, chelating, ligand has a marked effect in structural stability and allows for the tuning of electronic and steric features.[24] Such tuning also allows for multidrug resistance (MDR) to be tackled.[25] Indeed, most drugs act through apoptosis; compounds that are able to induce alternative forms of programmed cell death are therefore of high interest to bypass MDR. Such a redox activity can originate both from the metal and the ligands.[26–30] Additionally, chelating ligands have also been used as a scaffold for conjugation with biologically relevant molecules.[31–39]

Despite such promises, low selectivity of half-sandwich metal complexes for cancer cells is a challenge to overcome. In recent years, attempts to increase accumulation in cancer cells by conjugation of metal complexes with biological molecules such as proteins,[40–42] peptides,[43–46] or sugars[47] have been investigated. Glycoconjugation or functionalisation of drugs with carbohydrates has been shown to be a particularly promising approach for increasing the cellular uptake of a drug by cancer cells.[48–54] This strategy is based on the observation that tumour cells have increased proliferation rates and therefore re-

[+] These authors contributed equally to this work.
[#] Nicolas P. E. Barry, date of death: 16th of March 2023.
Supporting information for this article is available on the WWW under https://doi.org/10.1002/hlca.202300064

quire higher amount of glucose and other nutrients. Owing to the fast cell growth, cancer cells are known to perform anaerobic respiration to obtain energy which consumes glucose 10–100 times faster than normal oxidative phosphorylation (*Warburg* effect).[55] Numerous cancer cell lines have been shown to overexpress glucose transporters (GLUTs),[56,57] thus suggesting that addition of glucose-like substances can be used to attain specific delivery of drugs to tumour tissues. The dependence of glucose intake by cancer cells has already been used successfully to develop inorganic conjugates such as luminescent rhenium probes,[58,59] platinum,[49,52,60–64] or gold[65–67] chemotherapeutics and more recently with some ruthenium[68–70] and osmium[71–73] complexes.

Herein, we report on the synthesis and characterisation of five half-sandwich ruthenium and osmium dithiocarbamato isonipecotamide glycoconjugate complexes ([(η^6-*p*-cym)Ru(SSC-Inp-NH_2)] (**5**), [(η^6-*p*-cym)Os(SSC-Inp-NH_2)] (**6**), [(η^6-*p*-cym)Os(SSC-Inp-NHGlc1)] (**7**), [(η^6-*p*-cym)Os(SSC-Inp-NHGlc2)] (**8**), [(η^6-*p*-cym)Os(SSC-Inp-NHGlc3)] (**9**; *Figure 1*), synthesised from the corresponding zinc(II)-dithiocarbamato intermediates ([Zn(SSC-Inp-$NH_2)_2$] (**1**), [Zn(SSC-Inp-$NHGlc1)_2$] (**2**), [Zn(SSC-Inp-$NHGlc2)_2$] (**3**), [Zn(SSC-Inp-$NHGlc3)_2$] (**4**); *Figure 1*). The antiproliferative activity of the compounds towards ovarian cancer (A2780 and A2780cisR) and normal prostate (PNT2) cells is reported.

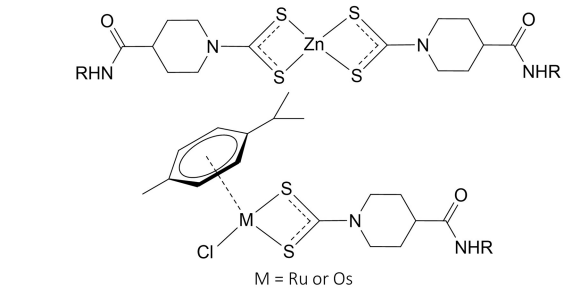

Compound	Metal centre	R
1	Zn (II)	H
2	Zn (II)	Glc1
3	Zn (II)	Glc2
4	Zn (II)	Glc3
5	Ru(II)	H
6	Os(II)	H
7	Os(II)	Glc1
8	Os(II)	Glc2
9	Os(II)	Glc3

Figure 1. Molecular structures of complexes **1**–**9**.

Results and Discussion

Synthesis and Characterisation

The dithiocarbamate ligands and the zinc(II) complexes **1**–**4** were prepared as previously described.[67] Complexes **5**–**9** were synthesised by a transmetallation reaction between the dichloro(η^6-*p*-cymene)metal(II) dimer with the zinc(II) complex bearing the corresponding dithiocarbamato isonipecotamide glycoconjugate ligand in DMF at ambient temperature (see *Experimental Section*). Attempts to use alternative solvents such as DMSO or THF resulted in low yields and high decomposition of the starting dimer. Similarly, increasing reaction times or heating resulted in decomposition products. Purification of the products was achieved by refluxing the compounds in acetonitrile with activated carbon for 10 min to remove reduced metal salts, followed by recrystallisation using a combination of acetonitrile and dichloromethane. All complexes were obtained in moderate-to-low yields.

The dithiocarbamato complexes **5**–**9** were characterised by ^{1}H-NMR spectroscopy and HR-ESI mass spectrometry (see *Figures S1–S13*). In (D_6)DMSO, two species are formed under such conditions, which correspond to the chlorido and DMSO adducts. Most of the peaks of both species overlap and we could not distinguish them. Furthermore, we could not identify which set of peaks corresponds to the chlorido or the DMSO adducts. A general upfield shift of the proton signals in the isonipecotamide linker can be observed for the Os(II) and Ru(II) compounds compared to the Zn(II). This is consistent with the increase of electron density at the metal centre which is experienced by the hydrogen atoms of the isonipecotate scaffold. As expected, the shift involves mainly the piperidine hydrogens, while the sugar ones remain unaffected by the change of metal in complexes **7**–**9**.

^{1}H-NMR spectra of complexes **8** and **9** demonstrate that transmetallation of the dithiocarbamato ligands from the Zn(II) analogues **3** and **4** gave rise to mainly the corresponding α-glycoconjugates. Such result is not unexpected as both complexes **3** and **4** contain the α-saccharide and anomerisation of the sugar is restricted by the methylation of the anomeric-hydroxyl (position C^1). However, in the case of complex **7**, a mixture of 3:5 β/α-anomers can be detected by ^{1}H-

NMR spectroscopy. The ratio β/α has increased significatively compared to 1:4 observed for complex **2**.

Figure 2 shows an example of the signal chemical shifts observed after transmetallation (complex **8** and its zinc precursor **3**).

IR Spectroscopy provided insights into the identification of the metal derivatives. As far as the dimer precursors $[(\eta^6\text{-}p\text{-cym})Ru^{II}Cl(\mu\text{-}Cl)]_2$ and $[(\eta^6\text{-}p\text{-cym})Os^{II}Cl(\mu\text{-}Cl)]_2$ are concerned, bands recorded in the mid-IR range resembled those observed for the free *p*-cymene ligand with minor changes in terms of $\tilde{\nu}_{max}$ and intensities, and were assigned according to previous literature reports.[74–77] On the contrary, in the far-IR region no significant bands were recorded for the isolated *p*-cymene scaffold as expected,[78] whereas new bands appeared in the spectra of both metal dimers. In particular, vibrations at 296 ($[(\eta^6\text{-}p\text{-cym})Ru^{II}Cl(\mu\text{-}Cl)]_2$)/316–304 ($[(\eta^6\text{-}p\text{-cym})Os^{II}Cl(\mu\text{-}Cl)]_2$) cm^{-1} and 262–244 ($[(\eta^6\text{-}p\text{-cym})Ru^{II}Cl(\mu\text{-}Cl)]_2$)/265 ($[(\eta^6\text{-}p\text{-cym})Os^{II}Cl(\mu\text{-}Cl)]_2$) cm^{-1} are undoubtedly assigned to the metal-terminal chloride and metal-bridging chloride stretching modes, respectively.[79–82] The metal-arene stretching vibrations are tentatively assigned to the new bands recorded in the 460–380 cm^{-1} based on the very few data reported in the literature for analogous organometallic scaffolds.[83,84]

The IR spectra of the various metal-dithiocarbamato derivatives present characteristic vibrations originated from the coordination of the dithiocarbamato scaffold following the zinc(II)-ruthenium(II)/osmium(II) transmetalation reaction. As an example, the mid-IR spectrum of the non-glycosylated osmium(II) complex $[(\eta^6\text{-}p\text{-cym})OsCl(SSC\text{-}Inp\text{-}NH_2)]$ (**6**) is shown in *Figure 3* and compared with those of the osmium(II) dimer precursor $[(\eta^6\text{-}p\text{-cym})Os^{II}Cl(\mu\text{-}Cl)]_2$ and the corresponding zinc(II) intermediate $[Zn(SSC\text{-}Inp\text{-}NH_2)_2]$ (**1**).

Although in the 4000–400 cm^{-1} range the main spectral features of the osmium dimer precursor and **1** are retained, some characteristic bands aided the identification of **6**. In particular, the strong band recorded at 1548 cm^{-1} can be undoubtedly attributed to the stretching vibration involving the dithiocarbamato moiety, ν(N-CSS). This band, which is shifted to higher energy compared with that observed for **1** (1492 cm^{-1}), is consistent with a chelating dithiocarbamato ligand coordinated to a metal centre.[85–87] Additionally, a shoulder is recorded at 1015 cm^{-1} and assigned to the antisymmetric stretching of the S–C–S moiety, which supports the presence of a bidentate dithiocarbamato group symmetrically coordinated to the metal centre.[88–90]

The bands recorded in the far-IR region provide useful information about the coordination sphere of the metal centres. As shown in *Figure 4*, the disappearance in the spectrum of **6** of the vibrations observed in the 350–500 cm^{-1} range for **1** (assigned to the $\nu_a(ZnS_4)$)[91,92] and at 316/304 cm^{-1} for the osmium dimer (assigned to the $\nu(Os\text{–}Cl_{bridging})$),[82] confirmed the successful replacement of the two bridging chlorides with the chelating dithiocarbamato ligand. This is also supported by the appearance of a new broad band at 386 cm^{-1} assigned to the $\nu_{a,s}(SOsS)$.[93]

Similar spectroscopic features and trends have also been observed for the other non-glycosylated ruthenium(II) counterpart $[(\eta^6\text{-}p\text{-cym})Ru^{II}Cl(SSC\text{-}Inp\text{-}NH_2)]$ (**5**), as well as for the glycoconjugate derivatives $[(\eta^6\text{-}p\text{-cym})Os^{II}Cl(SSC\text{-}Inp\text{-}NHGlc2)]$ (**8**) and $[(\eta^6\text{-}p\text{-cym})Os^{II}Cl(SSC\text{-}Inp\text{-}NHGlc3)]$ (**9**), the only differences being related to the bands specifically associated with

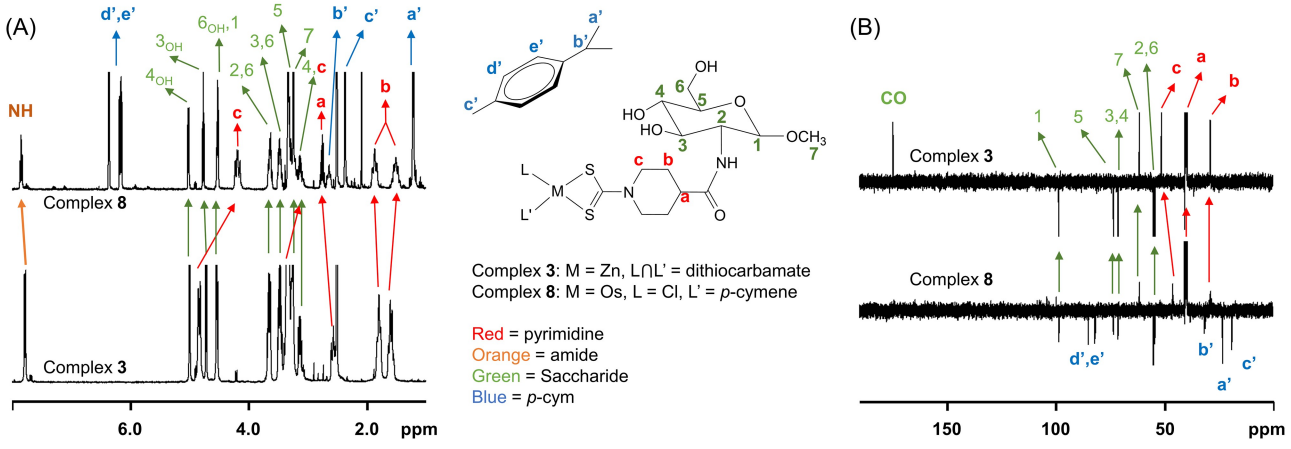

Figure 2. Comparison of the chemical shifts observed for complexes **3** and **8** by ^{1}H- and ^{13}C-NMR spectroscopy ($CDCl_3$).

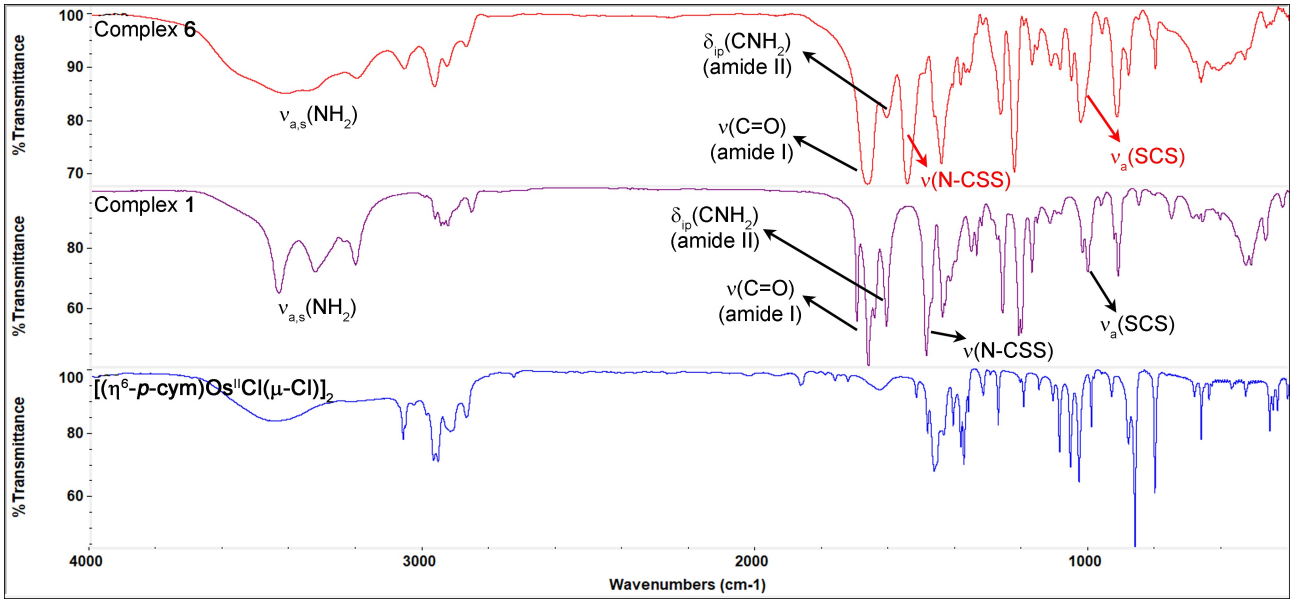

Figure 3. Comparison of the mid-IR spectra in CsI of [(η^6-*p*-cym)Os^{II}Cl(μ-Cl)]$_2$ (bottom), [Zn^{II}(SSC-Inp-NH$_2$)$_2$] (**1**; middle), and [(η^6-*p*-cym)Os^{II}Cl(SSC-Inp-NH$_2$)] (**6**; top).

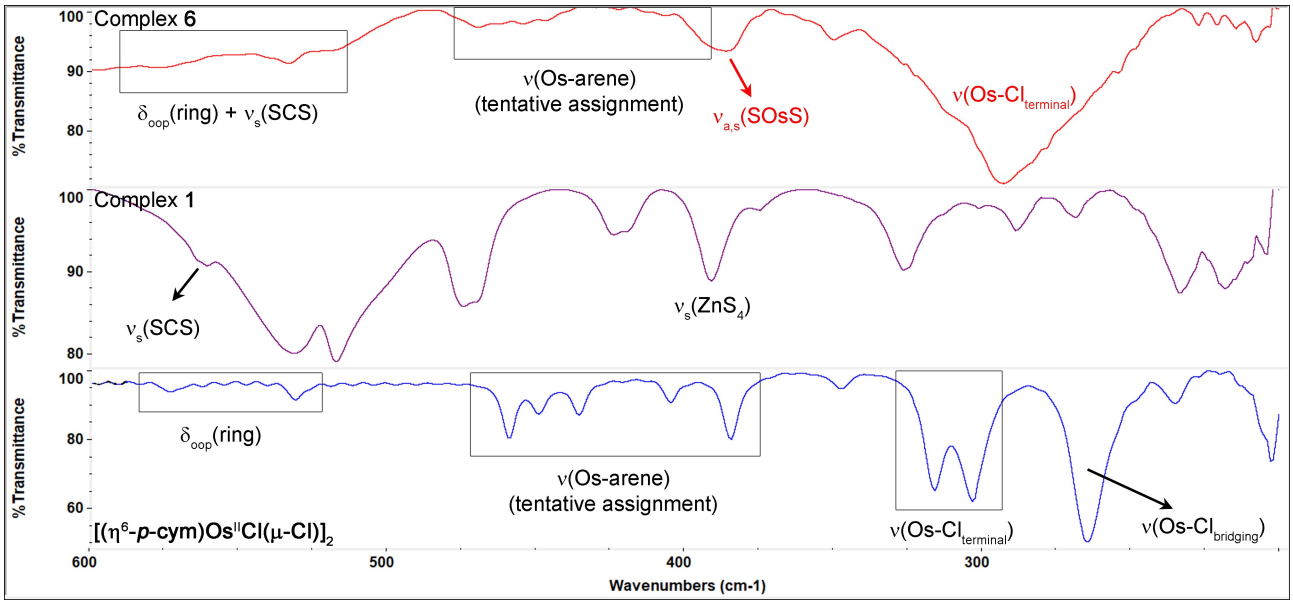

Figure 4. Comparison of the far-IR spectra in CsI of [(η^6-*p*-cym)Os^{II}Cl(μ-Cl)]$_2$ (bottom), [Zn^{II}(SSC-Inp-NH$_2$)$_2$] (**1**; middle), and [(η^6-*p*-cym)Os^{II}Cl(SSC-Inp-NH$_2$)] (**6**; top).

the various glucose-like scaffolds (see *Experimental Section* for detailed assignments and *Figures S14–S16* for the IR spectra).

DFT Calculations were used to determine the optimised structures of complexes **5**–**8** which confirmed the expected and typical piano-stool structure of dithiolato-containing half-sandwich metal complexes characterised by X-ray crystallography.[94,95] IR Spectra were computed using the time-dependent density functional theory method on the optimised structures using the same DFT functionals and basis sets in vacuum (see *Figure 5* and *Figures S14–S18* for the DFT-optimised structures and their calculated IR spectra).

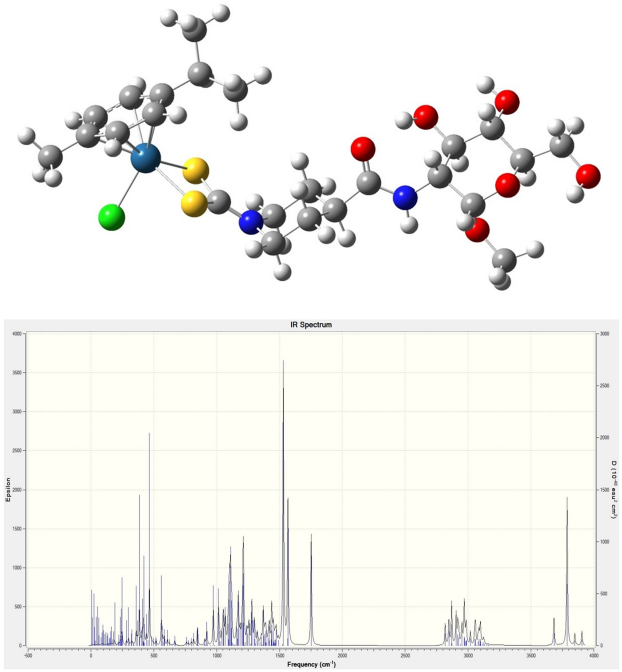

Figure 5. DFT-optimised structure of complex **7** in a tetrahydrofuran CPCM solvation model (light blue: osmium, yellow: sulphur, dark blue: nitrogen, red: oxygen, green: chloride, grey: carbon, white: hydrogen) and calculated IR spectrum.

Cytotoxicity Studies

The antiproliferative activity of the complexes against ovarian cancer cell lines A2780 and A2780cisR was studied, as well as in normal adult prostatic epithelial (PNT2) cells which were used as a model for non-cancerous cells, using a 24-hour MTT assay, with a 72-hour recovery period. Complexes **2** and **4** could not be tested owing to solubility issues, while compounds **1** and **3** were tested using 0.5% and 1% DMSO, respectively. The IC_{50} values obtained for all the complexes are shown in *Table 1*, together with the values for cisplatin which was used as a positive control.

All the compounds show IC_{50} values up to 20× higher than this of cisplatin. Additionally, loss of activity can be observed when using A2780cisR cell lines. However, despite the low activity in cancer cells, all the compounds were non-toxic to normal cells to a concentration of up to 300 μM. While this could be a hint at the selectivity towards cancer cells, the high IC_{50} values obtained on cancer cells prevent us from prematurely reaching such a conclusion. An improvement of the cytotoxicity and selectivity could be achieved by chemical modification of the complexes, for example by modification of the arene,[96,97] of the dithiocarbamato ligand,[98] or of the size of the metallacycle.[99,100] Zinc compounds **1** and **3** were shown to be slightly more active than their Os and Ru analogues.

Conclusions

In conclusion, five half-sandwich ruthenium and osmium complexes containing a 4-membered metallacycle were synthesised by transmetallation from the corresponding zinc precursors. and characterised. The metallacycle MS_2C was conjugated to a glucose-like moiety to study the influence of this bioactive moiety. The complexes were found to be very moderately active against A2780 ovarian cancer cells and A2780 cisplatin-resistant cell lines, with limited difference in the IC_{50} values against both cell lines, and therefore it seems likely there is no cross resistance. Of interest is the difference of IC_{50} values observed for the osmium complexes with or without the presence of the glucose-like moiety (complexes **7**–**9** *vs.* **6**). This confirms that glycoconjugation is an approach of

Table 1. IC_{50} values in A2780, A2780 cisplatin resistant and PNT2 cells for complexes **1**, **3**, **5**–**9**.

Compound	IC_{50} values [μM] A2780	A2780cisR	PNT2
1	109.44 ± 6.4	115.11 ± 29.8	NA
3	105.0 ± 0.84	111.07 ± 33.89	NA
5	146.8 ± 14.1**	194.2 ± 14.8	> 300
6	> 300	> 300	> 300
7	150.2 ± 11.1**	180.0 ± 11.1	> 300
8	173.6 ± 2.3**	213.9 ± 7.0	> 300
9	161.0 ± 5.8**	199.0 ± 1.9	> 300
cisplatin	7.7 ± 0.8 **	19.7 ± 1.4	77.3 ± 7.7

** $p < 0.01$ between A2780 and A2780CR.

interest for increasing the cellular uptake of a drug by cancer cells.

Experimental Section

Materials and Methods

Hydrated metallic chlorides were purchased from SA Precious Metals (South Africa, http://www.sapreciousmetals.com). The amino-sugar precursors 1-*O*-methyl-2-amino-2-deoxy-(α,β)-D-glucopyranoside (**Glc2**) acetic acid and 1-*O*-methyl-6-amino-6-deoxy-α-D-glucopyranoside (**Glc3**) were available in-house (prepared as previously described).[67] (α,β)-D-glucosamine (**GlcN1**) hydrochloride, isonipecotamide, isonipecotic acid (*TCI*), CS_2, $[Zn(OAc)_2]\cdot 2H_2O$, *N*,*N*-diisopropylethylamine (DIPEA; from *Merck*), *N*,*N*,*N*′,*N*′-tetramethyl-*O*-(*N*-succinimidyl)uronium tetrafluoroborate (TSTU; from *Carbosynth*) were of reagent grade or comparable purity and were used as supplied. Anhydrous DMF was obtained by passing the solvent over a column of alumina and subsequently stored over 4 Å activated molecular sieves under an inert atmosphere of nitrogen. Dichloromethane, tetrahydrofuran and toluene were dried over molecular sieves (3 Å). All other reagents and solvents were used as purchased without any further purification.

All Ru and Os compounds were prepared under a purified dinitrogen atmosphere using standard *Schlenk* and vacuum line techniques, unless otherwise specified.

pH* was adjusted using EDT direction non-glass pocket pH meter with an ISFET silicon chip pH sensor. pH* values (pH readings without correction for the effect of deuterium) of NMR samples were adjusted using KOD solutions in D_2O.

Instrumentation

All NMR spectra were recorded on a 400 MHz *Bruker Spectrospin* spectrometer or a *Jeol* 400 MHz spectrometer equipped with *z*-field gradients using 5 mm NMR tubes. Data processing was carried out using TOPSPIN 4.0.9 (*Bruker U.K. Ltd.*) and MestReNova version 12.0 (*Mestrelab Research S.L.*). Deuterated solvents were purchased from *Goss Scientific Instrument* or *Deutero*. ^{1}H- and ^{13}C-NMR chemical shifts were internally referenced to TMS through residual solvent peaks DMSO (δ = 2.52 ppm, 39.52 ppm), $CHCl_3$ (δ = 7.26 ppm, 77.16 ppm), acetone (δ = 2.05 ppm), THF (δ = 1.72 ppm) or MeOD (δ = 3.31 ppm).

Melting points were recorded on a *Stuart SMP10* digital melting point apparatus and are uncorrected.

Elemental analyses (carbon, hydrogen and nitrogen) were performed with a *Perkin Elmer 2400 CHNS/O Series II* analyser.

FT-IR Spectra were recorded from CsI disks at room temperature on a *Perkin Elmer Frontier FT-MIR/FIR* spectrophotometer in the range 4000–200 cm^{-1}. Data processing was carried out using OMNIC version 5.1 (*Nicolet Instrument Corporation*).

Roswell Park Memorial Institute (RPMI) 1640 medium, foetal bovine serum (FBS), penicillin and streptomycin, phosphate-buffered saline (PBS, pH 7.4), and other tissue culture reagents were purchased from *Gibco* (*Thermo Fisher Scientific*, UK). Cell lines were provided by the Institute of Cancer Therapeutics, University of Bradford. Cells were incubated in a *Thermo Scientific*™ *Heracell*™ *150* incubator and observed under a *Nikon ECLIPSE TS100* Microscope.

Geometry optimisations were carried out using the M11-L DFT functional[101] coupled with the SDD basis set[102] for the metal ions and the def2-TZVP basis set for the lighter elements.[103] Vibrational frequencies were calculated to ensure the absence of imaginary frequencies and to obtain the IR spectra. All calculations were performed in vacuum[104] and by utilising the Gaussian 09 software package.[105]

Synthesis and Characterisation

Ruthenium and osmium dimers $[(\eta^6\text{-}p\text{-cym})MCl_2]_2$ were synthesised using an *Anton Paar* microwave synthesis reactor (*Monowave 300*) and a 20 mL microwave vial equipped with a magnetic stirring bar.

$[(\eta^6\text{-}p\text{-cym})Ru^{II}Cl(\mu\text{-}Cl)]_2$. FT-IR (CsI disk; 298 K): 3058/3035 (ν, CH_{ar}), 2961 (ν_a, CH_3), 2925/2873 (ν_s, CH_3), 1628/1531/1497/1450/1410/1390 (ν, ring), 1472 (δ_a, CH_3), 1380/1363 (δ_s, CH_3), 1115/1094/1057/1034 (δ_{ip}, CH_{ar}), 928/904/879/804 (δ_{oop}, CH_{ar}), 571/528 (δ_{oop}, ring), 459–407 (ν, Ru-arene (tentative)), 296 (ν, $Ru\text{–}Cl_{terminal}$), 262/244 (ν, $Ru\text{–}Cl_{bridging}$).

$[(\eta^6\text{-}p\text{-cym})Os^{II}Cl(\mu\text{-}Cl)]_2$. FT-IR (CsI disk; 298 K): 3063/30555 (ν, CH_{ar}), 2971/2958 (ν_a, CH_3), 2921/2873

(ν_s, CH_3), 1630/1522/1487/1438/1411/1387 (ν, ring), 1467 (δ_a, CH_3), 1378/1362 (δ_s, CH_3), 1109/1091/1058/1032 (δ_{ip}, CH_{ar}), 935/883/864/804 (δ_{oop}, CH_{ar}), 573/531 (δ_{oop}, ring), 460–385 (ν, Os-arene (tentative)), 316/304 (ν, Os–$Cl_{terminal}$), 265/235 (ν, Os–$Cl_{bridging}$).

The zinc(II)-dithiocarbamato intermediates **1**–**4** were prepared as previously described.[67]

[Zn^{II}(SSC-Inp-NH_2)$_2$] (**1**). Yield: 96%. M.p. 293–294 °C (dec.). Anal. calc. for $C_{14}H_{22}N_4O_2S_4Zn$ (471.98): C 35.63, H 4.70, N 11.87; found: C 35.74, H 4.89, N 11.76. FT-IR (CsI disk; 298 K): 3439/3208 ($\nu_{a,s}$, NH_2), 1667 (ν, C=O (amide I)), 1649 (δ_{ip}, CNH_2 (amide II)), 1492 (ν, N–CSS), 1007 (ν_a, SCS), 561 (ν_s, SCS), 392 (ν_a, ZnS_4). ^{1}H-NMR (400 MHz; (D_6)DMSO; 298 K): 7.36 (2H, br. s, NH_{cis}), 6.87 (2H, br. s, NH_{trans}), 4.82 (4H, br. d, J=12.9, $C^{2',6'}H_{eq}$), 3.32–3.22 (4H, m, $C^{2',6'}H_{ax}$), 2.46–2.36 (2H, m, $C^{4'}H$), 1.82 (4H, dd, J=2.8, 13.2, $C^{3',5'}H_{eq}$), 1.54 (4H, m, $C^{3',5'}H_{ax}$). ^{13}C{^{1}H}-NMR (100 MHz; (D_6)DMSO; 298 K): 202.3 (NCSS), 175.6 (*C*=O), 50.7 ($C^{2',6'}H_2$), 40.1 ($C^{4'}$H), 28.4 ($C^{3',5'}H_2$).

[Zn^{II}(SSC-Inp-NHGlc1)$_2$] (**2**). Yield: 61%. M.p. 200–203 °C (dec.). Anal. calc. for $C_{26}H_{42}N_4O_{12}S_4Zn$ (796.26): C 39.22, H 5.32, N 7.04; found: C 39.18, H 5.19, N 6.91. FT-IR (CsI disk; 298 K): 3293_{br} (ν, OH+NH overlapped), 1638 (ν, C=O (amide I)), 1547 (δ_{ip}, CNH (amide II)), 1487 (ν, N–CSS), 1071_{br}/1060_{br} (ν, C–OH), 1005 (ν_a, SCS), 570 (ν_s, SCS), 373 (ν_a, ZnS_4). ^{1}H-NMR (400 MHz; (D_6)DMSO; 298 K): 7.70 (0.5H, d, J=8.3, N*H* β), 7.67 (2H, d, J=7.7, N*H* α), 6.49 (0.5H, d, J=6.3, C^1OH β), 6.41 (2H, d, J=4.2, C^1OH α), 4.94–4.90 (4H, m, C^3OH+C^1H α overlapped), 4.85–4.78 (5H, br. m, $C^{2',6'}H_{eq}$ α and β overlapped), 4.61 (2H, d, J=16.7, C^4OH α), 4.53 (0.5H, dd, J=5.80, 5.80, C^6OH β), 4.45–4.42 (2.5H, br. m, C^6OH α+C^1H β overlapped), 3.69–3.39 (11.5H, m, C^2H α+C^4H α and β+C^5H α+C^6H_2 α and β overlapped), 3.31–3.22 (6H, m, $C^{2',6'}H_{ax}$ α and β+C^2H β+C^3H β overlapped), 3.18–3.02 (2.5H, m, C^3H α+C^5H β overlapped), 2.57–2.52 (2.5H, m, $C^{4'}H$ α and β overlapped), 1.81–1.75 (5H, m, $C^{3',5'}H_{eq}$ α and β overlapped), 1.62–1.56 (5H, br. m, $C^{3',5'}H_{ax}$ α and β overlapped). C^3OH β and C^4OH β could not be undoubtedly assigned: those peaks are probably overlapped with other peaks in the 4.92–4.42 ppm range. ^{13}C{^{1}H}-NMR (100 MHz; (D_6)DMSO; 298 K): 202.2 (NCSS), 173.8 (*C*=O), 95.4 (C^1H β), 90.5 (C^1H α), 76.9 (C^5H β), 74.2 (C^3H β), 72.1 (C^5H α), 71.1 (C^3H α), 70.9 (C^4H β), 70.4 (C^4H α), 61.2 (C^6H_2 β), 61.1 (C^6H_2 α), 57.1 (C^2H β), 54.3 (C^2H α), 50.8 ($C^{2',6'}H_2$), 40.1 ($C^{4'}$H), 28.5 ($C^{3',5'}H_2$). No differentiation of the ^{13}C signals of the isonipecotic moiety due to the presence of both α and β anomers could be observed. Solution α:β anomers ratio *ca.* 4:1 (based on the ^{1}H-NMR spectrum).

[Zn^{II}(SSC-Inp-NHGlc2)$_2$] (**3**). Yield: 35%. M.p. 268–272 °C (dec.). Anal. calc. for $C_{28}H_{46}N_4O_{12}S_4Zn$ (824.31): C 40.80, H 5.63, N 6.80; found: C 40.65, H 5.74, N 6.81. FT-IR (CsI disk; 298 K): 3319_{br} (ν, OH+NH overlapped), 1645 (ν, C=O (amide I)), 1557 (δ_{ip}, CNH (amide II)), 1494 (ν, N–CSS), 1062_{br}/1040_{br} (ν, C–OH+C^1–O–CH_3 overlapped), 1007 (ν_a, SCS), 576 (ν_s, SCS), 382 (ν_a, ZnS_4). ^{1}H-NMR (400 MHz; (D_6)DMSO; 298 K): 7.80 (2H, d, J=8.1, N*H*), 5.00 (2H, d, J=5.6, C^4OH), 4.82 (4H, br. d, J=12.4, $C^{2',6'}H_{eq}$), 4.73 (2H, d, J=5.9, C^3OH), 4.56–4.52 (4H, m, C^6OH+C^1H overlapped), 3.67–3.42 (8H, m, $C^2H+C^3H+C^6H_2$ overlapped), 3.33–3.24 (6H, m, $C^5H+C^{2',6'}H_{ax}$ overlapped), 3.24 (6H, s, OCH_3), 3.15–3.09 (2H, m, C^4H), 2.59–2.52 (2H, m, $C^{4'}H$), 1.81–1.76 (4H, br. m, $C^{3',5'}H_{eq}$), 1.66–1.51 (4H, br. m, $C^{3',5'}H_{ax}$). The ^{1}H-NMR signals refer to the α anomer. Signals related to the β anomer were hardly detectable, and only a very few were observed and could be undoubtedly assigned (such as δ(N*H*)=7.68, $\delta(C^3OH)$=4.91, $\delta(C^1H)$=4.19 ($^3J_{1,2}$=8.4), $\delta(OCH_3)$=3.58 ppm). ^{13}C{^{1}H}-NMR (100 MHz; (D_6)DMSO; 298 K): 202.2 (NCSS), 173.9 (*C*=O), 97.9 (C^1H), 72.8 (C^5H), 70.8 (C^3H), 70.7 (C^4H), 60.9 (C^6H_2), 54.5 (OCH_3), 53.8 (C^2H), 50.8 ($C^{2',6'}H_2$), 40.0 ($C^{4'}$H), 28.5 ($C^{3',5'}H_2$). No ^{13}C signals assignable to the β anomer were detected. Solution α:β anomers ratio *ca.* 25:1 (based on the ^{1}H-NMR spectrum).

[Zn^{II}(SSC-Inp-NHGlc3)$_2$] (**4**). Yield: 76%. M.p. 245–248 °C (dec.). Anal. calc. for $C_{28}H_{46}N_4O_{12}S_4Zn$ (824.31): C 40.80, H 5.63, N 6.80; found: C 40.91, H 5.83, N 6.76. FT-IR (CsI disk; 298 K): 3392_{br} (ν, OH+NH overlapped), 1637 (ν, C=O (amide I)), 1543 (δ_{ip}, CNH (amide II)), 1494 (ν, N–CSS), 1050_{br} (ν, C–OH+C^1–O–CH_3 overlapped), 1010 (ν_a, SCS), 564 (ν_s, SCS), 366 (ν_a, ZnS_4). ^{1}H-NMR (400 MHz; (D_6)DMSO; 298 K): 7.97 (2H, dd, J=5.8, 5.8, N*H*), 4.97 (2H, d, J=5.5, C^4OH), 4.90–4.80 (4H, br. m, $C^{2',6'}H_{eq}$), 4.82 (2H, d, J=4.8, C^3OH), 4.75 (2H, d, J=6.5, C^2OH), 4.51 (2H, d, J=3.6, C^1H), 3.58–3.52 (2H, m, C^6H'), 3.40–3.35 (4H, m, C^3H+C^5H overlapped), 3.24 (6H, s, OCH_3), 3.28–3.19 (6H, m, $C^2H+C^{2',6'}H_{ax}$ overlapped), 3.08–2.98 (2H, m, C^6H''), 2.92–2.88 (2H, m, C^4H), 2.57–2.53 (2H, m, $C^{4'}H$), 1.78–1.75 (4H, m, $C^{3',5'}H_{eq}$), 1.67–1.50 (4H, br. m, $C^{3',5'}H_{ax}$). ^{13}C{^{1}H}-NMR (100 MHz; (D_6)DMSO; 298 K): 202.2 (NCSS), 173.8 (*C*=O), 99.6 (C^1H), 73.0 (C^3H), 72.1 (C^4H), 72.0 (C^2H), 70.3 (C^5H), 54.3 (OCH_3), 50.7 ($C^{2',6'}H_2$), 39.9 ($C^{4'}$H), 39.8 (C^6H_2), 28.4 ($C^{3',5'}H_2$).

[(*p*-cym)Ru(SSC-Inp-NH_2)Cl] (**5**). A suspension of **1** (71.0 mg, 0.16 mmol) in dry DMF (2 mL) was added dropwise to a solution of ruthenium dimer [(*p*-cym)$RuCl_2]_2$ (100 mg, 0.16 mmol) in dry DMF (2 mL). The mixture was then stirred at room temperature until no precipitate could be observed (1 h) and the solution turned from turbid orange to clear red. Slow addition of diethyl ether resulted in the formation of a red/brown precipitate which was discarded. A second addition of diethyl ether (100 mL) resulted in the precipitation of the crude compound as an orange powder. The residue was subsequently washed with diethyl ether and dried under vacuum. The orange powder was then dissolved in acetonitrile and refluxed in the presence of activated carbon for 10 min before filtration through *Celite*. The final product was purified by precipitation in acetonitrile/dichloromethane. Yield: 36.03 %. HR-ESI-MS (pos.): 439.04505 ($[M-Cl]^+$; calc. 439.045172; mass error: −0.278 ppm). FT-IR (CsI disk; 298 K): 3421/3347_{sh}/3196 ($\nu_{a,s}$, NH_2), 3058 (ν, CH_{ar}), 2966 (ν_a, CH_3), 2930/2872 (ν_s, CH_3), 1670 (ν, C=O (amide I)), 1614 (δ_{ip}, CNH_2 (amide II)), 1542 (ν, N–CSS), 1500/1446 (overlapped with $\delta_a(CH_3)$)/1390 (ν, ring), 1362 (δ_s, CH_3), 1117/1092/1057/1028 (δ_{ip}, CH_{ar}), 1018_{sh} (ν_a, SCS), 965/917/881/802 (δ_{oop}, CH_{ar}), 598/535 (δ_{oop}, ring, overlapped with ν_s(SCS)), 455–394 (ν, Ru-arene (tentative)), 376/362 ($\nu_{a,s}$, SRuS), 294 (ν, Ru-$Cl_{terminal}$). ^{1}H-NMR (400 MHz; (D_6)DMSO; 298 K): 7.32 (1H, 2 s, NH_{cis} and N^*H_{cis}), 6.84 (1H, 2 s, NH_{trans} and N^*H_{trans}), 6.24–6.14 (2H, m, $C^{e'}H$), 6.00 (1H, d, J=6.4, $C^{*d'}H$), 5.97 (1H, d, J=6.4, $C^{d'}H$), 4.30–4.22 (2H, m, C^cH_{eq}), 3.22–3.14 (2H, m, C^cH_{ax}), 2.72 (1H, sept, J=6.9, $C^{b'}H$), 2.54–2.48 (1H, m, C^aH), 2.18 (3H, 2 s, $C^{c'}H$ and $C^{*c'}H$), 1.86–1.73 (2H, m, C^bH_{eq}), 1.51–1.27 (2H, m, C^bH_{ax}), 1.14 (6H, d, J=6.9, 2 $C^{a'}H_3$). $^{13}C\{^1H\}$-NMR (100 MHz; (D_6)DMSO; 298 K): 91.5 ($C^{d'}H$), 88.9 ($C^{e'}H$), 46.0 ($C^{*c}H_2$), 45.9 (C^cH_2), 30.8 (C^aH), 28.0 ($C^{*b}H_2$), 27.6 (C^bH_2), 22.3 ($C^{a'}H_3$), 22.2 ($C^{a'}H_3$),18.4 ($C^{c'}H_3$). Two species are formed with the majority of the signals overlapping. Distinguishable signals are marked with a * for the second species.

[(*p*-cym)Os(SSC-Inp-NH_2)Cl] (**6**). Complex **6** was synthesised following the procedure described above for complex **5**. Yield: 33.7 %. HR-ESI-MS (pos.): 529.10217 ($[M-Cl]^+$; calc. 529.102319;mass error −0.282 ppm). FT-IR (CsI disk; 298 K): 3414/3342_{sh}/3196 ($\nu_{a,s}$, NH_2), 3058 (ν, CH_{ar}), 2968 (ν_a, CH_3), 2931/2874 (ν_s, CH_3), 1668 (ν, C=O (amide I)), 1610 (δ_{ip}, CNH_2 (amide II)), 1548 (ν, N–CSS), 1467/1446 (overlapped with $\delta_a(CH_3)$)/1388 (ν, ring), 1363 (δ_s, CH_3), 1116/1089/1055/1028 (δ_{ip}, CH_{ar}), 1015_{sh} (ν_a, SCS), 962/918/883/802 (δ_{oop}, CH_{ar}), 577/534 (δ_{oop}, ring, overlapped with ν_s(SCS)), 470–390 (ν, Os-arene (tentative)), 386_{br} ($\nu_{a,s}$, SOsS), 293 (ν, Os-$Cl_{terminal}$). ^{1}H-NMR (400 MHz; (D_6)DMSO; 298 K): 7.37 (1H, 2 s, NH_{cis} and N^*H_{cis}), 6.95–6.87 (1H, m, NH_{trans} and N^*H_{trans}), 6.35 (2H, d, J=5.9, $C^{e'}H$), 6.16 (1H, d, J=6.1, $C^{*d'}H$), 6.14 (1H, d, J=6.1, $C^{d'}H$), 4.23–4.10 (2H, m, C^cH_{eq}), 3.31–3.18 (2H, m, C^cH_{ax}), 2.73 (1H, sept, J=6.8, $C^{b'}H$), 2.49–2.44 (1H, m, C^aH), 2.36 (3H, 2 s, $C^{c'}H$ and $C^{*c'}H$), 1.94–1.84 (2 H, m, C^bH_{eq}), 1.58–1.38 (2H, m, C^bH_{ax}), 1.20 (6H, d, J=7.0, 2 $C^{a'}H_3$). Two species are formed with the majority of the signals overlapping. Distinguishable signals are marked with a * for the second species.

[(*p*-cym)Os(SSC-Inp-NHGlc1)Cl] (**7**). Complex **7** was synthesised following the procedure described above for complex **5**. Yield: 28.8 %. HR-ESI-MS (pos.): 705.16951 ($[M-Cl]^+$; calc. 705.170793; mass error −1.819 ppm). FT-IR (CsI disk; 298 K): 3435_{br} (ν, OH+NH overlapped), 3061/3029 (ν, CH_{ar}), 2961 (ν_a, CH_3), 2923/2868 (ν_s, CH_3), 1655 (ν, C=O (amide I)), 1544 (ν, N–CSS), 1504 (δ_{ip}, CNH (amide II)), 1463/1447 (overlapped with $\delta_a(CH_3)$)/1410/1387 (ν, ring), 1371 (δ_s, CH_3), 1120/1086 (δ_{ip}, CH_{ar}), 1039/1056 (ν, C–OH+C^1–O–CH_3 overlapped), 1008_{sh} (ν_a, SCS), 918/880/802 (δ_{oop}, CH_{ar}), 577/532 (δ_{oop}, ring, overlapped with ν_s(SCS)), 463–397 (ν, Os-arene (tentative)), 380_{br} ($\nu_{a,s}$, SOsS), 295 (ν, Os–$Cl_{terminal}$). ^{1}H-NMR (400 MHz; (D_6)DMSO; 298 K): 7.89–7.74 (1H, m, NH), 6.38–6.29 (2H, m, $C^{e'}H$), 6.17 (1H, d, J=6.3, $C^{*d'}H$), 6.14 (1H, d, J=6.3, $C^{d'}H$), 5.02–4.97 (1H, m, C^4OH), 4.76–4.70 (1H, m, C^3OH), 4.54–4.47 (2H, m, C^6OH and C^1H), 4.23–4.10 (2H, m, C^cH_{eq}), 3.67–3.56 (2H, m, C^2H and C^6H), 3.50–3.41 (2H, m, C^3H and C^6H), 3.27–3.07 (10H, m, C^5H, C^cH_{ax}, C^7H, C^4H, and OCH_3), 2.75 (1H, sept, J=7.1, $C^{b'}H$), 2.67–2.57 (1H, m, C^aH), 2.38–2.32 (3H, m, $C^{*c'}H$ and $C^{c'}H$), 1.91–1.78 (2H, m, C^bH_{eq}), 1.58–1.40 (2H, m, C^bH_{ax}), 1.21 (6H, d, J=7.1, $C^{a'}H$). Two species are formed with the majority of the signals overlapping. Distinguishable signals are marked with a * for the second species. The ^{1}H-NMR signals refer to the α anomer. Signals related to the β anomer were hardly detectable. $^{13}C\{^1H\}$-NMR (100 MHz; (D_6)DMSO; 298 K): 200.35 (NCS_2), 97.81 (C^1H), 84.30 ($C^{e'}H$), 81.30 ($C^{*d'}H$), 81.04 ($C^{d'}H$), 72.76 (C^5H), 70.74 (C^4H), 70.61 (C^3H), 60.77 (C^6H_2), 54.41 (C^7H_3), 53.73 (C^2H), 45.66 (C^cH_2), 39.78 (C^aH_3), 30.98 ($C^{b'}H$), 28.27 (C^bH_2), 22.72 ($C^{a'}H_3$), 18.48 ($C^{c'}H_3$).

[(*p*-cym)Os(SSC-Inp-NHGlc2)Cl] (**8**). Complex **8** was synthesised following the procedure described above for complex **5**. Yield: 29.5 %. HR-ESI-MS (pos.): 691.15313 ($[M-Cl]^+$; calc. 691.155144; mass error

−2.914 ppm). FT-IR (CsI disk; 298 K): 3414/3342$_{sh}$/3196 ($\nu_{a,s}$, NH_2), 3058 (ν, CH_{ar}), 2968 (ν_a, CH_3), 2931/2874 (ν_s, CH_3), 1668 (ν, C=O (amide I)), 1610 (δ_{ip}, CNH_2 (amide II)), 1548 (ν, N–CSS), 1467/1446 (overlapped with $\delta_a(CH_3)$)/1388 (ν, ring), 1363 (δ_s, CH_3), 1116/1089/1055/1028 (δ_{ip}, CH_{ar}), 1015$_{sh}$ (ν_a, SCS), 962/918/883/802 (δ_{oop}, CH_{ar}), 577/534 (δ_{oop}, ring, overlapped with ν_s(SCS)), 470–390 (ν, Os-arene (tentative)), 386$_{br}$ ($\nu_{a,s}$, SOsS), 293 (ν, Os–$Cl_{terminal}$). ^{1}H-NMR (400 MHz; (D_6)DMSO; 298 K): 8.04–7.92 (1H, m, NH), 6.38–6.30 (3H, m, $C^{e'}H$), 6.16 (1H, d, J=6.5, $C^{*d'}H$), 6.14 (1H, d, J=6.5, $C^{d'}H$), 4.98–4.95 (1H, m, C^4OH), 4.84–4.80 (1 H, m, C^3OH), 4.76–4.73 (1H, m, C^6OH), 4.52–4.49 (1H, m, C^1H), 4.23–4.12 (2H, m, C^cH_{eq}), 3.61–2.95 (9H, m, C^1OH, C^2H, C^3H, C^4H, C^5H, C^6H_2, C^cH_{ax}), 2.75 (1H, sept, J=6.9, $C^{b'}H$), 2.63–2.55 (1H, m, C^aH), 2.36 (3H, 2s, $C^{*c'}H$, $C^{c'}H$), 1.91–1.77 (2H, m, C^bH_{eq}), 1.59–1.41 (2H, m, C^bH_{ax}), 1.21 (6H, d, J=7.1, $C^{a'}H$). Two species formed for each anomer with majority of the signals overlapping between them. Distinguishable signals are marked with a * for the second specie. $^{13}C\{^1H\}$-NMR (100 MHz; (D_6)DMSO; 298 K): 199.60 (NCS_2), 95.43 (C^1H), 90.50 ($C^{e'}H$), 76.86 ($C^{d'}H$), 72.12 (C^5H), 71.10 (C^4H), 70.41 (C^3H), 61.11 (C^6H_2), 54.31 (C^2H), 50.77 (C^cH_2), 33.00 ($C^{b'}H$), 28.40 (C^bH_2), 24.01 ($C^{a'}H_3$), 20.59 ($C^{c'}H_3$).

[(*p*-cym)Os(SSC-Inp-NHGlc3)Cl] (**9**). Complex **9** was synthesised following the procedure described above for complex **5**. Yield: 13.7%. HR-ESI-MS (pos.): 705.16884 ([*M*−Cl]$^+$; calc. 705.170793; mass error −2.770 ppm). FT-IR (CsI disk; 298 K): 3435$_{br}$ (ν, OH+NH overlapped), 3057 (ν, CH_{ar}), 2961 (ν_a, CH_3), 2928/2869 (ν_s, CH_3), 1654 (ν, C=O (amide I)), 1546 (ν, N–CSS), 1503 (δ_{ip}, CNH (amide II)), 1466/1446 (overlapped with $\delta_a(CH_3)$)/1409/1388 (ν, ring), 1371 (δ_s, CH_3), 1148/1107/1085 (δ_{ip}, CH_{ar}), 1051 (ν, C–OH+C^1–O–CH_3 overlapped), 1010 (ν_a, SCS), 918/878/801 (δ_{oop}, CH_{ar}), 568/537 (δ_{oop}, ring, overlapped with ν_s(SCS)), 456–396 (ν, Os-arene (tentative)), 383$_{br}$ ($\nu_{a,s}$, SOsS), 294 (ν, Os–$Cl_{terminal}$). ^{1}H-NMR (400 MHz; (D_6)DMSO; 298 K): 7.77–7.61 (1H, m, NH), 6.35 (2H, d, J=6.3, $C^{e'}H$), 6.16 (1H, d, J=6.03, $C^{*d'}H$), 6.14 (1H, d, J=6.03, $C^{d'}H$), 4.99–4.75 (2H, m, C^3OH and C^4OH), 4.65–4.59 (1H, m, C^2OH), 4.47–4.38 (1H, m, C^1H), 4.24–4.07 (2H, m, C^cH_{eq}), 3.70–2.99 (11H, m, C^2H, C^3H, C^4H, C^5H, C^6H_2, C^cH_{ax}, OCH_3), 2.73 (1H, sept, J=6.9, $C^{b'}H$), 2.69–2.64 (1H, m, C^aH), 2.40–2.34 (3H, m, $C^{c'}H$), 2.34–2.29 (3H, m, $C^{*c'}H$), 1.93–1.78 (2H, m, C^bH_{eq}), 1.62–1.40 (2H, m, C^bH_{ax}), 1.21 (6H, d, J=6.4, $C^{a'}H$). Two species formed with majority of the signals overlapping. Distinguishable signals are marked with a * for the second specie. The ^{1}H-NMR signals refer to the α anomer.

Chemosensitivity Assays

In vitro chemosensitivity tests were performed against A2780, A2780cisR and PNT2 cells. Cancer cell lines were routinely maintained as monolayer cultures in RPMI medium supplemented with 10% foetal calf serum, penicillin (100 I.U./mL), streptomycin (100 μg/mL), sodium pyruvate (1 mm), and L-glutamine (2 mm). For chemosensitivity studies, cells were incubated in 96-well plates at a concentration of 7.5×103 cells per well and the plates were incubated for 24 h at 37 °C and a 5% CO_2 humidified atmosphere prior to drug exposure. Complexes were dissolved in DMSO to provide stock solutions which were further diluted with media to provide a range of final concentrations. Drug-media solutions were added to cells (the final concentration of DMSO was less than 1% (*v/v*) in all cases) and incubated for 24 h at 37 °C and 5% CO_2 humidified atmosphere. The drug-media was removed from the wells and the cells were washed with PBS (100 μL, twice), and 100 μL of complete fresh media were added to each well. The plates were further incubated for 48 h at 37 °C in a 5% CO_2 humidified atmosphere to allow for a period of recovery. 3-(4,5-dimethylthiazol-2-yl)-2,5-diphenyltetrazolium bromide (MTT; 20 μL, 2.5 mg/mL) was added to each well and incubated for 2 h at 37 °C and 5% CO_2 humidified atmosphere. All solutions were then removed and 100 μL of DMSO was added to each well in order to dissolve the purple formazan crystals. A *Thermo Scientific Multiskan EX* microplate photometer was used to measure the absorbance in each well at 570 nm. Cell survival was determined as the absorbance of treated cells divided by the absorbance of controls and expressed as a percentage. The IC_{50} values were determined from plots of % survival against drug concentration. Each experiment was repeated in triplicates of triplicates and a mean value was obtained and stated as IC_{50} [μM] ± SD. Cisplatin was also used as a positive control.

Acknowledgements

This project was supported by *The Royal Society* (University Research Fellowship No. UF150295 to *N.P.E.B.*), the University of Bradford, the Academy of Medical Sciences/the Wellcome Trust/the Government Department of Business, Energy and Industrial Strat-

egy/the British Heart Foundation Springboard Award (SBF003\1170 to N.P.E.B.), and by the CNRS and the Université Paris-Saclay. Financial support by the University of Galway (*College of Science Scholarship 2014* to A.P.; *Millennium Fund Minor Project 2013* to *L. Ro.*) and the Irish Research Council (*Postgraduate Scholarship GOIPG/2015/2961* to *A.P.*) is gratefully acknowledged. Financial support from the Romanian Ministry of Education and Research is gratefully acknowledged. The computational facilities were provided by the Babeş-Bolyai University under project POC/398/1/1/124155 – co-financed by the European Regional Development Fund (ERDF) through the Competitiveness Operational Program for Romania 2014-2020.

Data Availability Statement

The data that support the findings of this study are available from the corresponding author upon reasonable request.

Author Contribution Statement

A. P.-B., *L. Ro.*, and *N. P. E. B.* designed the project idea. *J. J. S.-B.*, *A. P.*, *A. P.-B.* synthesised and characterised the materials. *N. P. E. B.* and *J. J. S.-B.* designed the *in vitro* experiments. *J. J. S.-B.*, *M. A.*, and *L. Ro.* performed the *in vitro* experiments. *A. L.* and *A. A. A. A.* designed and performed the theoretical experiments. The paper was written through contributions of *J. J. S.-B.*, *A. L.*, *L. Ra.*, *N. P. E. B.*, and *A. P.-B.* All authors have given approval to the final version of the paper.

References

[1] Z. Liu, I. Romero-Canelón, B. Qamar, J. M. Hearn, A. Habtemariam, N. P. E. Barry, A. M. Pizarro, G. J. Clarkson, P. J. Sadler, 'The Potent Oxidant Anticancer Activity of Organoiridium Catalysts', *Angew. Chem. Int. Ed.* **2014**, *53*, 3941–3946.

[2] A. A. Nazarov, C. G. Hartinger, P. J. Dyson, 'Opening the lid on piano-stool complexes: An account of ruthenium(II)–arene complexes with medicinal applications', *J. Organomet. Chem.* **2014**, *751*, 251–260.

[3] A. M. Pizarro, N. P. E. Barry, P. J. Sadler, 'Metal–DNA Coordination Complexes', in 'Comprehensive Inorganic Chemistry II', Vol. 3, Ed. J. Reedijk, Elsevier, 2013, 751–784.

[4] C. S. Allardyce, P. J. Dyson, D. J. Ellis, S. L. Heath, '[Ru(η^6-*p*-cymene)Cl_2 (pta)] (pta = 1,3,5-triaza-7-phosphatricyclo-[3.3.1.1]decane): a water soluble compound that exhibits pH dependent DNA binding providing selectivity for diseased cells', *Chem. Commun.* **2001**, 1396–1397.

[5] S. Chatterjee, S. Kundu, A. Bhattacharyya, C. G. Hartinger, P. J. Dyson, 'The ruthenium(II)–arene compound RAPTA-C induces apoptosis in EAC cells through mitochondrial and p53–JNK pathways', *J. Biol. Inorg. Chem.* **2008**, *13*, 1149–1155.

[6] T.-T. Thai, B. Therrien, G. Süss-Fink, 'Arene ruthenium oxinato complexes: Synthesis, molecular structure and catalytic activity for the hydrogenation of carbon dioxide in aqueous solution', *J. Organomet. Chem.* **2009**, *694*, 3973–3981.

[7] W. H. Ang, A. Casini, G. Sava, P. J. Dyson, 'Organometallic ruthenium-based antitumor compounds with novel modes of action', *J. Organomet. Chem.* **2011**, *696*, 989–998.

[8] J. Lemke, N. Metzler-Nolte, 'Organometallic peptide NHC complexes of Cp Rh(III) and arene Ru(II) moieties from L-thiazolylalanine', *J. Organomet. Chem.* **2011**, *696*, 1018–1022.

[9] S. J. Lucas, R. M. Lord, R. L. Wilson, R. M. Phillips, V. Sridharan, P. C. McGowan, 'Synthesis of iridium and ruthenium complexes with (*N*,*N*), (*N*,*O*) and (*O*,*O*) coordinating bidentate ligands as potential anti-cancer agents', *Dalton Trans.* **2012**, *41*, 13800–13802.

[10] Y. Fu, C. Sanchez-Cano, R. Soni, I. Romero-Canelon, J. M. Hearn, Z. Liu, M. Wills, P. J. Sadler, 'The contrasting catalytic efficiency and cancer cell antiproliferative activity of stereoselective organoruthenium transfer hydrogenation catalysts', *Dalton Trans.* **2016**, *45*, 8367–8378.

[11] T. Völker, E. Meggers, 'Chemical Activation in Blood Serum and Human Cell Culture: Improved Ruthenium Complex for Catalytic Uncaging of Alloc-Protected Amines', *ChemBioChem* **2017**, *18*, 1083–1086.

[12] F. Chen, I. Romero-Canelón, J. J. Soldevila-Barreda, J.-I. Song, J. P. C. Coverdale, G. J. Clarkson, J. Kasparkova, A. Habtemariam, M. Wills, V. Brabec, P. J. Sadler, 'Transfer Hydrogenation and Antiproliferative Activity of Tethered Half-Sandwich Organoruthenium Catalysts', *Organometallics* **2018**, *37*, 1555–1566.

[13] S. M. Meier-Menches, C. Gerner, W. Berger, C. G. Hartinger, B. K. Keppler, 'Structure–activity relationships for ruthenium and osmium anticancer agents – towards clinical development', *Chem. Soc. Rev.* **2018**, *47*, 909–928.

[14] N. Mohan, M. K. M. Subarkhan, R. Ramesh, 'Synthesis, antiproliferative activity and apoptosis-promoting effects of arene ruthenium(II) complexes with N, O chelating ligands', *J. Organomet. Chem.* **2018**, *859*, 124–131.

[15] J.-C. Chen, Y. Zhang, X.-M. Jie, J. She, G.-Z. Dongye, Y. Zhong, Y.-Y. Deng, J. Wang, B.-Y. Guo, L.-M. Chen, 'Ruthenium(II) salicylate complexes inducing ROS-mediated apoptosis by targeting thioredoxin reductase', *J. Inorg. Biochem.* **2019**, *193*, 112–123.

[16] J. Li, Z. Tian, X. Ge, Z. Xu, Y. Feng, Z. Liu, 'Design, synthesis, and evaluation of fluorine and Naphthyridine–Based half-sandwich organoiridium/ruthenium complexes with bioimaging and anticancer activity', *Eur. J. Med. Chem.* **2019**, *163*, 830–839.

[17] M. Hanif, M. V. Babak, C. G. Hartinger, 'Development of anticancer agents: wizardry with osmium', *Drug Discovery Today* **2014**, *19*, 1640–1648.

[18] C. A. Riedl, L. S. Flocke, M. Hejl, A. Roller, M. H. M. Klose, M. A. Jakupec, W. Kandioller, B. K. Keppler, 'Introducing the 4-Phenyl-1,2,3-Triazole Moiety as a Versatile Scaffold for the Development of Cytotoxic Ruthenium(II) and Osmium(II) Arene Cyclometalates', *Inorg. Chem.* **2017**, *56*, 528–541.
[19] A. F. A. Peacock, A. Habtemariam, R. Fernández, V. Walland, F. P. A. Fabbiani, S. Parsons, R. E. Aird, D. I. Jodrell, P. J. Sadler, 'Tuning the Reactivity of Osmium(II) and Ruthenium(II) Arene Complexes under Physiological Conditions', *J. Am. Chem. Soc.* **2006**, *128*, 1739–1748.
[20] W. F. Schmid, R. O. John, V. B. Arion, M. A. Jakupec, B. K. Keppler, 'Highly Antiproliferative Ruthenium(II) and Osmium(II) Arene Complexes with Paullone-Derived Ligands', *Organometallics* **2007**, *26*, 6643–6652.
[21] I. Romero-Canelón, L. Salassa, P. J. Sadler, 'The Contrasting Activity of Iodido versus Chlorido Ruthenium and Osmium Arene Azo- and Imino-pyridine Anticancer Complexes: Control of Cell Selectivity, Cross-Resistance, p53 Dependence, and Apoptosis Pathway', *J. Med. Chem.* **2013**, *56*, 1291–1300.
[22] J. P. C. Coverdale, I. Romero-Canelón, C. Sanchez-Cano, G. J. Clarkson, A. Habtemariam, M. Wills, P. J. Sadler, 'Asymmetric transfer hydrogenation by synthetic catalysts in cancer cells', *Nat. Chem.* **2018**, *10*, 347–354.
[23] J. J. Soldevila-Barreda, M. Azmanova, A. Pitto-Barry, P. A. Cooper, S. D. Shnyder, N. P. E. Barry, 'Preclinical Anticancer Activity of an Electron-Deficient Organoruthenium(II) Complex', *ChemMedChem* **2020**, *15*, 982–987.
[24] A. Habtemariam, M. Melchart, R. Fernández, S. Parsons, I. D. H. Oswald, A. Parkin, F. P. A. Fabbiani, J. E. Davidson, A. Dawson, R. E. Aird, D. I. Jodrell, P. J. Sadler, 'Structure–Activity Relationships for Cytotoxic Ruthenium(II) Arene Complexes Containing N,N-, N,O-, and O,O-Chelating Ligands', *J. Med. Chem.* **2006**, *49*, 6858–6868.
[25] M. J. Chow, C. Licona, G. Pastorin, G. Mellitzer, W. H. Ang, C. Gaiddon, 'Structural tuning of organoruthenium compounds allows oxidative switch to control ER stress pathways and bypass multidrug resistance', *Chem. Sci.* **2016**, *7*, 4117–4124.
[26] N. Nayeem, M. Contel, 'Exploring the Potential of Metallodrugs as Chemotherapeutics for Triple Negative Breast Cancer', *Chem. Eur. J.* **2021**, *27*, 8891–8917.
[27] Z. Fan, J. Huang, H. Huang, S. Banerjee, 'Metal-Based Catalytic Drug Development for Next-Generation Cancer Therapy', *ChemMedChem* **2021**, *16*, 2480–2486.
[28] C. Gaiddon, I. Gross, X. Meng, M. Sidhoum, G. Mellitzer, B. Romain, J.-B. Delhorme, A. Venkatasamy, A. C. Jung, M. Pfeffer, 'Bypassing the Resistance Mechanisms of the Tumor Ecosystem by Targeting the Endoplasmic Reticulum Stress Pathway Using Ruthenium- and Osmium-Based Organometallic Compounds: An Exciting Long-Term Collaboration with Dr. Michel Pfeffer', *Molecules* **2021**, *26*, 5386.
[29] P. Chellan, P. J. Sadler, 'Enhancing the Activity of Drugs by Conjugation to Organometallic Fragments', *Chem. Eur. J.* **2020**, *26*, 8676–8688.
[30] P. Zhang, P. J. Sadler, 'Redox-Active Metal Complexes for Anticancer Therapy', *Eur. J. Inorg. Chem.* **2017**, 1541–1548.
[31] P. Štarha, Z. Trávníček, 'Non-platinum complexes containing releasable biologically active ligands', *Coord. Chem. Rev.* **2019**, *395*, 130–145.
[32] R. Hudej, J. Kljun, W. Kandioller, U. Repnik, B. Turk, C. G. Hartinger, B. K. Keppler, D. Miklavčič, I. Turel, 'Synthesis and Biological Evaluation of the Thionated Antibacterial Agent Nalidixic Acid and Its Organoruthenium(II) Complex', *Organometallics* **2012**, *31*, 5867–5874.
[33] F. Aman, M. Hanif, M. Kubanik, A. Ashraf, T. Söhnel, S. M. F. Jamieson, W. A. Siddiqui, C. G. Hartinger, 'Anti-Inflammatory Oxicams as Multi-donor Ligand Systems: pH- and Solvent-Dependent Coordination Modes of Meloxicam and Piroxicam to Ru and Os', *Chem. Eur. J.* **2017**, *23*, 4893–4902.
[34] J. Kljun, I. E. León, Š. Peršič, J. F. Cadavid-Vargas, S. B. Etcheverry, W. He, Y. Bai, I. Turel, 'Synthesis and biological characterization of organoruthenium complexes with 8-hydroxyquinolines', *J. Inorg. Biochem.* **2018**, *186*, 187–196.
[35] M. Patra, G. Gasser, 'The medicinal chemistry of ferrocene and its derivatives', *Nat. Chem. Rev.* **2017**, *1*, 0066.
[36] L. Biancalana, L. K. Batchelor, A. De Palo, S. Zacchini, G. Pampaloni, P. J. Dyson, F. Marchetti, 'A general strategy to add diversity to ruthenium arene complexes with bioactive organic compounds *via* a coordinated (4-hydroxyphenyl)diphenylphosphine ligand', *Dalton Trans.* **2017**, *46*, 12001–12004.
[37] S. Banerjee, A. R. Chakravarty, 'Metal Complexes of Curcumin for Cellular Imaging, Targeting, and Photoinduced Anticancer Activity', *Acc. Chem. Res.* **2015**, *48*, 2075–2083.
[38] J. J. Soldevila-Barreda, K. B. Fawibe, M. Azmanova, L. Rafols, A. Pitto-Barry, U. B. Eke, N. P. E. Barry, 'Synthesis, Characterisation and In Vitro Anticancer Activity of Catalytically Active Indole-Based Half-Sandwich Complexes', *Molecules* **2020**, *25*, 4540.
[39] V. C. Nolan, L. Rafols, J. Harrison, J. J. Soldevila-Barreda, M. Crosatti, N. J. Garton, M. Wegrzyn, D. L. Timms, C. C. Seaton, H. Sendron, M. Azmanova, N. P. E. Barry, A. Pitto-Barry, J. A. G. Cox, 'Indole-containing arene-ruthenium complexes with broad spectrum activity against antibiotic-resistant bacteria', *Curr. Res. Microb. Sci.* **2022**, *3*, 100099.
[40] L. Li, J. Rousseau, M. D. G. Jaraquemada-Peláez, X. Wang, A. Robertson, V. Radchenko, P. Schaffer, K.-S. Lin, F. Bénard, C. Orvig, '^{225}Ac-H$_4$py4pa for Targeted Alpha Therapy', *Bioconjugate Chem.* **2021**, *32*, 1348–1363.
[41] S. M. Meier-Menches, A. Casini, 'Design Strategies and Medicinal Applications of Metal-Peptidic Bioconjugates', *Bioconjugate Chem.* **2020**, *31*, 1279–1288.
[42] J. Han, A. F. B. Räder, F. Reichart, B. Aikman, M. N. Wenzel, B. Woods, M. Weinmüller, B. S. Ludwig, S. Stürup, G. M. M. Groothuis, H. P. Permentier, R. Bischoff, H. Kessler, P. Horvatovich, A. Casini, 'Bioconjugation of Supramolecular Metallacages to Integrin Ligands for Targeted Delivery of Cisplatin', *Bioconjugate Chem.* **2018**, *29*, 3856–3865.
[43] D. Obitz, R. G. Miller, N. Metzler-Nolte, 'Synthesis and DNA interaction studies of Ru(II) cell penetrating peptide (CPP) bioconjugates', *Dalton Trans.* **2021**, *50*, 13768–13777.
[44] C. S. Burke, A. Byrne, T. E. Keyes, 'Highly Selective Mitochondrial Targeting by a Ruthenium(II) Peptide

Conjugate: Imaging and Photoinduced Damage of Mitochondrial DNA', *Angew. Chem. Int. Ed.* **2018**, *57*, 12420–12424.
[45] F. Gayraud, M. Klußmann, I. Neundorf, 'Recent Advances and Trends in Chemical CPP–Drug Conjugation Techniques', *Molecules* **2021**, *26*, 1591.
[46] L. C.-C. Lee, A. W.-Y. Tsang, H.-W. Liu, K. K.-W. Lo, 'Photofunctional Cyclometalated Iridium(III) Polypyridine Complexes Bearing a Perfluorobiphenyl Moiety for Bioconjugation, Bioimaging, and Phototherapeutic Applications', *Inorg. Chem.* **2020**, *59*, 14796–14806.
[47] M. Martínez-Alonso, G. Gasser, 'Ruthenium polypyridyl complex-containing bioconjugates', *Coord. Chem. Rev.* **2021**, *434*, 213736.
[48] E. C. Calvaresi, P. J. Hergenrother, 'Glucose conjugation for the specific targeting and treatment of cancer', *Chem. Sci.* **2013**, *4*, 2319–2333.
[49] A. Annunziata, M. E. Cucciolito, R. Esposito, P. Imbimbo, G. Petruk, G. Ferraro, V. Pinto, A. Tuzi, D. M. Monti, A. Merlino, F. Ruffo, 'A highly efficient and selective antitumor agent based on a glucoconjugated carbene platinum(II) complex', *Dalton Trans.* **2019**, *48*, 7794–7800.
[50] Y. Wang, S. Ma, Z. Dai, Z. Rong, J. Liu, 'Facile *In Situ* synthesis of ultrasmall near-infrared-emitting gold glyconanoparticles with enhanced cellular uptake and tumor targeting', *Nanoscale* **2019**, *11*, 16336–16341.
[51] T. Itoh, K. Tamura, H. Ueda, T. Tanaka, K. Sato, R. Kuroda, S. Aoki, 'Design and synthesis of boron containing monosaccharides by the hydroboration of D-glucal for use in boron neutron capture therapy (BNCT)', *Bioorg. Med. Chem.* **2018**, *26*, 5922–5933.
[52] M. Patra, S. G. Awuah, S. J. Lippard, 'Chemical Approach to Positional Isomers of Glucose–Platinum Conjugates Reveals Specific Cancer Targeting through Glucose-Transporter-Mediated Uptake *In Vitro* and *In Vivo*', *J. Am. Chem. Soc.* **2016**, *138*, 12541–12551.
[53] J. Fu, J. Yang, P. H. Seeberger, J. Yin, 'Glycoconjugates for glucose transporter-mediated cancer-specific targeting and treatment', *Carbohydr. Res.* **2020**, *498*, 108195.
[54] J. Matović, J. Järvinen, H. C. Bland, I. K. Sokka, S. Imlimthan, R. M. Ferrando, K. M. Huttunen, J. Timonen, S. Peräniemi, O. Aitio, A. J. Airaksinen, M. Sarparanta, M. P. Johansson, J. Rautio, F. S. Ekholm, 'Addressing the Biochemical Foundations of a Glucose-Based "Trojan Horse"-Strategy to Boron Neutron Capture Therapy: From Chemical Synthesis to *In Vitro* Assessment', *Mol. Pharmaceutics* **2020**, *17*, 3885–3899.
[55] M. V. Liberti, J. W. Locasale, 'The Warburg Effect: How Does it Benefit Cancer Cells?', *Trends Biochem. Sci.* **2016**, *41*, 211–218.
[56] F. Hossain, P. R. Andreana, 'Developments in Carbohydrate-Based Cancer Therapeutics', *Pharmaceuticals* **2019**, *12*, 84.
[57] P.-B. Ancey, C. Contat, E. Meylan, 'Glucose transporters in cancer – from tumor cells to the tumor microenvironment', *FEBS J.* **2018**, *285*, 2926–2943.
[58] K. Y. Zhang, K. K.-S. Tso, M.-W. Louie, H.-W. Liu, K. K.-W. Lo, 'A Phosphorescent Rhenium(I) Tricarbonyl Polypyridine Complex Appended with a Fructose Pendant That Exhibits Photocytotoxicity and Enhanced Uptake by Breast Cancer Cells', *Organometallics* **2013**, *32*, 5098–5102.
[59] M.-W. Louie, H.-W. Liu, M.-H. C. Lam, Y.-W. Lam, K. K.-W. Lo, 'Luminescent Rhenium(I) Polypyridine Complexes Appended with an α-D-Glucose Moiety as Novel Biomolecular and Cellular Probes', *Chem. Eur. J.* **2011**, *17*, 8304–8308.
[60] A. Annunziata, A. Amoresano, M. E. Cucciolito, R. Esposito, G. Ferraro, I. Iacobucci, P. Imbimbo, R. Lucignano, M. Melchiorre, M. Monti, C. Scognamiglio, A. Tuzi, D. M. Monti, A. Merlino, F. Ruffo, 'Pt(II) versus Pt(IV) in Carbene Glycoconjugate Antitumor Agents: Minimal Structural Variations and Great Performance Changes', *Inorg. Chem.* **2020**, *59*, 4002–4014.
[61] M. Patra, T. C. Johnstone, K. Suntharalingam, S. J. Lippard, 'A Potent Glucose–Platinum Conjugate Exploits Glucose Transporters and Preferentially Accumulates in Cancer Cells', *Angew. Chem. Int. Ed.* **2016**, *55*, 2550–2554.
[62] C. G. Hartinger, A. A. Nazarov, S. M. Ashraf, P. J. Dyson, B. K. Keppler, 'Carbohydrate-Metal Complexes and their Potential as Anticancer Agents', *Curr. Med. Chem.* **2008**, *15*, 2574–2591.
[63] J. Ma, Q. Wang, Z. Huang, X. Yang, Q. Nie, W. Hao, P. G. Wang, X. Wang, 'Glycosylated Platinum(IV) Complexes as Substrates for Glucose Transporters (GLUTs) and Organic Cation Transporters (OCTs) Exhibited Cancer Targeting and Human Serum Albumin Binding Properties for Drug Delivery', *J. Med. Chem.* **2017**, *60*, 5736–5748.
[64] C. Bischin, A. Lupan, V. Taciuc, R. Silaghi-Dumitrescu, 'Interactions Between Proteins and Platinum-Containing Anti-Cancer Drugs', *Mini-Rev. Med. Chem.* **2011**, *11*, 214–224.
[65] A. Pettenuzzo, K. Vezzù, M. L. Di Paolo, E. Fotopoulou, L. Marchiò, L. Della Via, L. Ronconi, 'Design, physico-chemical characterization and *In Vitro* biological activity of organogold(III) glycoconjugates', *Dalton Trans.* **2021**, *50*, 8963–8979.
[66] A. Pettenuzzo, R. Pigot, L. Ronconi, 'Metal-based glycoconjugates and their potential in targeted anticancer chemotherapy', *Metallodrugs* **2015**, *1*, 36–61.
[67] A. Pettenuzzo, D. Montagner, P. McArdle, L. Ronconi, 'An innovative and efficient route to the synthesis of metal-based glycoconjugates: proof-of-concept and potential applications', *Dalton Trans.* **2018**, *47*, 10721–10736.
[68] L. N. Lameijer, J. le Roy, S. van der Vorm, S. Bonnet, 'Synthesis of *O*-1–*O*-6 Substituted Positional Isomers of D-Glucose–Thioether Ligands and Their Ruthenium Polypyridyl Conjugates', *J. Org. Chem.* **2018**, *83*, 12985–12997.
[69] C. A. Fernandes, 'Synthesis, Biological Activity and Medicinal Applications of Ruthenium Complexes Containing Carbohydrate Ligands', *Curr. Med. Chem.* **2019**, *26*, 6412–6437.
[70] G. Bononi, D. Iacopini, G. Cicio, S. Di Pietro, C. Granchi, V. Di Bussolo, F. Minutolo, 'Glycoconjugated Metal Complexes as Cancer Diagnostic and Therapeutic Agents', *ChemMedChem* **2021**, *16*, 30–64.
[71] P. R. Florindo, D. M. Pereira, P. M. Borralho, P. J. Costa, M. F. M. Piedade, C. M. P. Rodrigues, A. C. Fernandes, 'New $[(\eta^5\text{-}C_5H_5)Ru(N{-}N)(PPh_3)][PF_6]$ compounds: colon anticancer activity and GLUT-mediated cellular uptake of

carbohydrate-appended complexes', *Dalton Trans.* **2016**, *45*, 11926–11930.
[72] D. Pallarola, N. Queralto, W. Knoll, M. Ceolín, O. Azzaroni, F. Battaglini, 'Redox-Active Concanavalin A: Synthesis, Characterization, and Recognition-Driven Assembly of Interfacial Architectures for Bioelectronic Applications', *Langmuir* **2010**, *26*, 13684–13696.
[73] R. Cerón-Camacho, M. A. Roque-Ramires, A. D. Ryabov, R. Le Lagadec, 'Cyclometalated Osmium Compounds and beyond: Synthesis, Properties, Applications', *Molecules* **2021**, *26*, 1563.
[74] N. P. E. Barry, R. J. Deeth, G. J. Clarkson, I. Prokes, P. J. Sadler, 'Thermochromic organometallic complexes: experimental and theoretical studies of 16- to 18-electron interconversions of adducts of arene Ru(II) carboranes with aromatic amine ligands', *Dalton Trans.* **2013**, *42*, 2580–2587.
[75] D. Lin-Vien, N. B. Colthup, W. G. Fateley, J. G. Grasselli, 'Aromatic and Heteroaromatic Rings', in 'The Handbook of Infrared and Raman Characteristic Frequencies of Organic Molecules', Eds. D. Lin-Vien, N. B. Colthup, W. G. Fateley, J. G. Grasselli), Academic Press, San Diego, 1991, Chapt. 17, pp. 277–306.
[76] F. Marszaukowski, I. D. L. Guimarães, J. P. da Silva, L. H. da Silveira Lacerda, S. R. de Lazaro, M. P. de Araujo, P. Castellen, T. T. Tominaga, R. T. Boeré, K. Wohnrath, 'Ruthenium(II)-arene complexes with monodentate aminopyridine ligands: Insights into redox stability and electronic structures and biological activity', *J. Organomet. Chem.* **2019**, *881*, 66–78.
[77] J. Masternak, A. Gilewska, K. Kazimierczuk, O. V. Khavryuchenko, J. Wietrzyk, J. Trynda, B. Barszcz, 'Synthesis, physicochemical and theoretical studies on new rhodium and ruthenium dimers. Relationship between structure and cytotoxic activity', *Polyhedron* **2018**, *154*, 263–274.
[78] Y. P. Bazhenov, L. Z. Kas'yanova, A. I. Bokin, B. I. Kutepov, A. N. Khazipova, E. A. Travkin, N. A. Shchadneva, R. I. Khusnutdinov, U. M. Dzhemilev, 'Hydrogenation and Skeleton Rearrangements of α-Pinene on Heterogeneous Catalysts', *Russ. J. Appl. Chem.* **2003**, *76*, 234–237.
[79] M. A. Bennett, T.-N. Huang, T. W. Matheson, A. K. Smith, S. Ittel, W. Nickerson, '16. (η^6-Hexamethylbenzene) Ruthenium Complexes', in 'Inorganic Syntheses', Vol. 21, 1982, pp. 74–78.
[80] R. A. Zelonka, M. C. Baird, 'Benzene Complexes of Ruthenium(II)', *Can. J. Chem.* **1972**, *50*, 3063–3072.
[81] G. Winkhaus, H. Singer, 'Ruthen(II)-komplexe mit zweizähnigem cycloheptatrien und benzol', *J. Organomet. Chem.* **1967**, *7*, 487–491.
[82] L. Vaska, 'Hydridocarbonyl Complexes of Osmium by Reaction with Alcohols', *J. Am. Chem. Soc.* **1964**, *86*, 1943–1950.
[83] K. Nakamoto, in 'Infrared and Raman Spectra of Inorganic and Coordination Compounds', John Wiley & Sons, Hoboken, 2009, p. 314.
[84] T. Polzer, A. Ellebracht, W. Kiefer, U. Wecker, H. Werner, 'Novel synthesis and vibrational analysis of (arene)-osmium(II) complexes of the type $[(C_6H_3(CH_3)_3)OsH_2(L)]$', *J. Organomet. Chem.* **1992**, *438*, 319–328.
[85] A. E. Gallio, L. Brustolin, N. Pettenuzzo, D. Fregona, 'Binuclear Heteroleptic Ru(III) Dithiocarbamate Complexes: A Step towards Tunable Antiproliferative Agents', *Inorganics* **2022**, *10*, 37.
[86] Y.-H. Dou, S.-D. Xu, Y. Chen, X.-H. Wu, 'Synthesis, characterization, and anticancer activity of dithiocarbamate ruthenium(II) complexes', *Phosphorus Sulfur Silicon Relat. Elem.* **2017**, *192*, 1219–1223.
[87] S. Naeem, A. L. Thompson, A. J. P. White, L. Delaude, J. D. E. T. Wilton-Ely, 'Dithiocarboxylate complexes of ruthenium(II) and osmium(II)', *Dalton Trans.* **2011**, *40*, 3737–3747.
[88] S. Sobczak, K. Roszak, A. Katrusiak, 'Exchanged Metal-Hydrogen Anagostic Bonds and Resonance of Dithiocarbamate and Thioureide Mesomers', *Chem. Eur. J.* **2022**, *28*, e202201235.
[89] C. Preti, G. Tosi, P. Zannini, 'Synthesis and characterization of ruthenium dithiocarbamate complexes', *J. Inorg. Nucl. Chem.* **1979**, *41*, 485–488.
[90] R. Kellner, G. S. Nikolov, N. Trendafilova, 'Detecting the bonding type of dithiocarbamate ligands in their complexes as inferred from the asymmetric CS mode', *Inorg. Chim. Acta* **1984**, *84*, 233–239.
[91] L.-N. Liu, J.-G. Dai, T.-J. Zhao, S.-Y. Guo, D.-S. Hou, P. Zhang, J. Shang, S. Wang, S. Han, 'A novel Zn(II) dithiocarbamate/ZnS nanocomposite for highly efficient Cr^{6+} removal from aqueous solutions', *RSC Adv.* **2017**, *7*, 35075–35085.
[92] R. Kellner, G. S. Nikolov, 'Far IR spectra of dithiocarbamate complexes correlations with structure parameters', *J. Inorg. Nucl. Chem.* **1981**, *43*, 1183–1188.
[93] D. C. Bradley, M. H. Gitlitz, 'Preparation and properties of *NN*-dialkyldithiocarbamates of early transition elements', *J. Chem. Soc. A* **1969**, 1152–1156.
[94] M. Azmanova, L. Rafols, P. A. Cooper, C. C. Seaton, S. D. Shnyder, A. Pitto-Barry, 'Anticancer Water-Soluble Organoruthenium Complexes: Synthesis and Preclinical Evaluation', *ChemBioChem* **2022**, *23*, e202200259.
[95] W.-G. Jia, Y.-F. Han, J.-S. Zhang, G.-X. Jin, 'Synthesis and characterization of half-sandwich Ir and Ru complexes containing Mnt ligand (Mnt = maleonitriledithiolate)', *Inorg. Chem. Commun.* **2007**, *10*, 1222–1225.
[96] S. Infante-Tadeo, V. Rodríguez-Fanjul, A. Habtemariam, A. M. Pizarro, 'Osmium(II) tethered half-sandwich complexes: pH-dependent aqueous speciation and transfer hydrogenation in cells', *Chem. Sci.* **2021**, *12*, 9287–9297.
[97] J. P. Mészáros, V. F. S. Pape, G. Szakács, G. Németi, M. Dénes, T. Holczbauer, N. V. May, É. A. Enyedy, 'Half-sandwich organometallic Ru and Rh complexes of (N,N) donor compounds: effect of ligand methylation on solution speciation and anticancer activity', *Dalton Trans.* **2021**, *50*, 8218–8231.
[98] L. Giovagnini, S. Sitran, I. Castagliuolo, P. Brun, M. Corsini, P. Zanello, A. Zoleo, A. Maniero, B. Biondi, D. Fregona, 'Ru(III)-based compounds with sulfur donor ligands: synthesis, characterization, electrochemical behaviour and anticancer activity', *Dalton Trans.* **2008**, 6699–6708.
[99] A. Pitto-Barry, A. Lupan, M. Zegke, T. Swift, A. A. A. Attia, R. M. Lord, N. P. E. Barry, 'Pseudo electron-deficient organometallics: limited reactivity towards electron-donating ligands', *Dalton Trans.* **2017**, *46*, 15676–15683.
[100] I. Romero-Canelón, B. Phoenix, A. Pitto-Barry, J. Tran, J. J. Soldevila-Barreda, N. Kirby, S. Green, P. J. Sadler, N. P. E.

Barry, 'Arene ruthenium dithiolato–carborane complexes for boron neutron capture therapy (BNCT)', *J. Organomet. Chem.* **2015**, *796*, 17–25.
[101] R. Peverati, D. G. Truhlar, 'M11-L: A Local Density Functional That Provides Improved Accuracy for Electronic Structure Calculations in Chemistry and Physics', *J. Phys. Chem. Lett.* **2012**, *3*, 117–124.
[102] A. Nicklass, M. Dolg, H. Stoll, H. Preuss, '*Ab initio* energy-adjusted pseudopotentials for the noble gases Ne through Xe: Calculation of atomic dipole and quadrupole polarizabilities', *J. Chem. Phys.* **1995**, *102*, 8942–8952.
[103] F. Weigend, R. Ahlrichs, 'Balanced basis sets of split valence, triple zeta valence and quadruple zeta valence quality for H to Rn: Design and assessment of accuracy', *Phys. Chem. Chem. Phys.* **2005**, *7*, 3297–3305.
[104] M. Cossi, N. Rega, G. Scalmani, V. Barone, 'Energies, structures, and electronic properties of molecules in solution with the C-PCM solvation model', *J. Comput. Chem.* **2003**, *24*, 669–681.
[105] G. W. T. M. J. Frisch, H. B. Schlegel, G. E. Scuseria, M. A. Robb, J. R. Cheeseman, G. Scalmani, V. Barone, G. A. Petersson, H. Nakatsuji, X. Li, M. Caricato, A. Marenich, J. Bloino, B. G. Janesko, R. Gomperts, B. Mennucci, H. P. Hratchian, J. V. Ortiz, A. F. Izmaylov, J. L. Sonnenberg, D. Williams-Young, F. Ding, F. Lipparini, F. Egidi, J. Goings, B. Peng, A. Petrone, T. Henderson, D. Ranasinghe, V. G. Zakrzewski, J. Gao, N. Rega, G. Zheng, W. Liang, M. Hada, M. Ehara, K. Toyota, R. Fukuda, J. Hasegawa, M. Ishida, T. Nakajima, Y. Honda, O. Kitao, H. Nakai, T. Vreven, K. Throssell, J. A. Montgomery Jr., J. E. Peralta, F. Ogliaro, M. Bearpark, J. J. Heyd, E. Brothers, K. N. Kudin, V. N. Staroverov, T. Keith, R. Kobayashi, J. Normand, K. Raghavachari, A. Rendell, J. C. Burant, S. S. Iyengar, J. Tomasi, M. Cossi, J. M. Millam, M. Klene, C. Adamo, R. Cammi, J. W. Ochterski, R. L. Martin, K. Morokuma, O. Farkas, J. B. Foresman, D. J. Fox, Gaussian, Inc., Wallingford CT, 2016.

Received April 18, 2023
Accepted July 5, 2023